

Impact of annealing atmosphere on the multiferroic and dielectric properties of $\text{BiFeO}_3/\text{Bi}_{3.25}\text{La}_{0.75}\text{Ti}_3\text{O}_{12}$ thin films

Fengzhen Huang · Xiaomei Lu · Zhe Wang · Weiwei Lin · Yi Kan · Huifeng Bo ·
Wei Cai · Jinsong Zhu

Received: 25 May 2009 / Accepted: 10 June 2009 / Published online: 27 June 2009
© Springer-Verlag 2009

Abstract Multiferroic $\text{BiFeO}_3/\text{Bi}_{3.25}\text{La}_{0.75}\text{Ti}_3\text{O}_{12}$ films annealed in different atmospheres (N_2 or O_2) were prepared on $\text{Pt}/\text{Ti}/\text{SiO}_2/\text{Si}$ substrates via a metal organic decomposition method. Based on our experimental results, it is considered that, in the films annealed in N_2 , fewer Fe^{2+} ions while more oxygen vacancies are involved. As a result, at room temperature, predominated by the reduced Fe^{2+} fraction, lower leakage current and dielectric loss, better ferroelectric property while reduced magnetization are observed. However, the oxygen vacancies might be thermally activated at elevated temperature; thus, more strongly temperature-dependent leakage current and a higher dielectric relaxation peak are observed for the films annealed in N_2 .

PACS 77.22.Gm · 75.80.+q · 81.15.-z

1 Introduction

Multiferroics are promising materials for the design and synthesis of multifunctional devices [1–3]. They are noteworthy for their unique and strong coupling of electric, magnetic and structural order parameters, giving rise to simultaneous (anti)ferroelectricity, (anti)ferromagnetism and/or ferroelasticity [4, 5]. As one of the most important single-phase multiferroic materials, BiFeO_3 (BFO) has attracted much attention because it has both a higher ferroelectric

Curie temperature of about 1103 K and an antiferromagnetic Néel temperature of about 643 K [3]. The combined action of exchange and spin-orbit interactions produces spin canting away from perfect antiferromagnetic ordering, which results in a macroscopic magnetization in thin films and nanoparticles, while a vanishing magnetization in the bulk [6].

However, complicated synthesis of pure BFO and its large leakage current have hampered its practical applications [7, 8]. It was reported that the processing conditions played a decisive role in the properties of BFO [9, 10]. The oxygen pressure at a fixed deposition temperature predominated the crystallinity and the electric properties of BFO films synthesized by pulsed laser deposition [11]. As for the BFO films prepared by the chemical solution deposition (CSD) method, the annealing atmosphere also plays an important role. Yun et al. [12] and Singh et al. [13] reported that the BFO films annealed in N_2 possessed pure perovskite phase and superior properties, while those annealed in O_2 and air showed the formation of secondary phases. Although similar results were obtained in the BFO films annealed in air, Iakovlev et al. [14] found that the films annealed in O_2 could also acquire pure perovskite phases. Up to now, the exact impact of annealing atmosphere on the structural and physical properties of BFO as well as the real mechanism inside it are still unclear. Thus, in this paper, we try to find why BFO behaves differently under different annealing atmospheres (N_2 or O_2) by investigating carefully the oxidation states of Fe, the amount of oxygen vacancies, the leakage current and the multiferroic and dielectric properties of $\text{BFO}/\text{Bi}_{3.25}\text{La}_{0.75}\text{Ti}_3\text{O}_{12}$ (BLT) films, in which BLT is introduced only as a buffer layer as discussed in our former paper [15].

F. Huang · X. Lu (✉) · Z. Wang · W. Lin · Y. Kan · H. Bo ·
W. Cai · J. Zhu

National Laboratory of Solid State Microstructures, Physics
Department, Nanjing University, Nanjing 210093, People's
Republic of China
e-mail: xiaomeil@nju.edu.cn
Fax: +86-25-83595535

2 Experimental details

BFO/BLT thin films were fabricated on (111) Pt/Ti/SiO₂/Si substrates by a metal organic decomposition (MOD) method [15]. A BLT film with a thickness of about 200 nm was first spin coated on the substrates and then crystallized at 700°C in O₂. Subsequently, a BFO layer also of about 200 nm in thickness was deposited on the BLT film and crystallized at 550°C in N₂ and O₂, respectively. To measure the electrical properties of the films, Pt top electrodes were deposited by sputtering through a shadow mask. X-ray diffraction (XRD, D/Max-RB) with Cu K_α radiation and atomic force microscopy (AFM, Nanoscope III) were used for the structural analysis. The combination states of Fe 2p, O 1s and N 1s electrons were examined by X-ray photoelectron spectroscopy (XPS, ESCALab MK-II). The leakage current was measured by a Keithley 6517A electrometer, while the dielectric characteristics were evaluated using a HP4194 impedance analyzer in the frequency range from 1 kHz to 1 MHz and the temperature range from 300 to 680 K. The ferroelectric and magnetic hysteresis loops of the samples were analyzed at room temperature by a RT66A standard ferroelectric test unit and a vibrating sample magnetometer (EV7, ADE, USA), respectively. For the sake of conciseness, in the following, BFON is used to represent the BFO/BLT films with the BFO layer annealed in N₂, while BFOO represents the samples with the BFO layer annealed in O₂.

3 Results and discussion

Figure 1 shows the X-ray diffraction patterns of the BFON and BFOO films. Similar spectra with pure phase polycrystalline structure are observed for the two films, which indicate that different annealing atmospheres (N₂ or O₂) have no obvious influence on the crystalline structure of the films

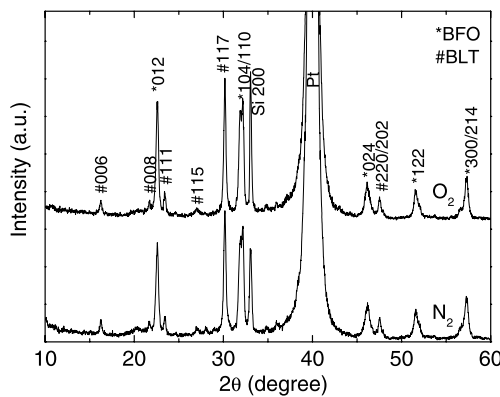


Fig. 1 X-ray diffraction patterns of the BFON and BFOO films

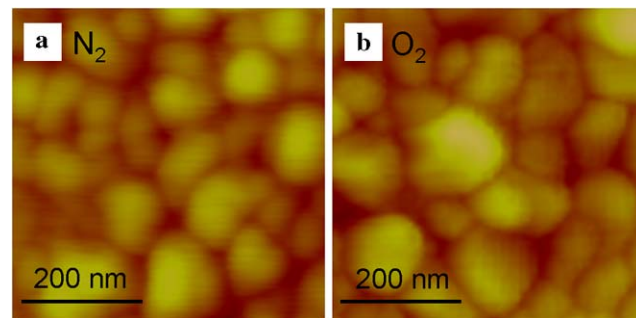


Fig. 2 AFM topography of **a** the BFON and **b** the BFOO films

within the uncertainty of XRD. Moreover, the surface morphologies of the two films (Fig. 2) are also alike, with the average grain size being about 100 nm.

The room-temperature magnetic and ferroelectric properties are different for the two films annealed in different atmospheres. Both of the two films show a saturated weak ferromagnetic response (Fig. 3a), and the saturation magnetization M_s is reduced for the BFON films. Figure 3b shows the ferroelectric hysteresis loops of the two films; unlike the result in the epitaxial films [16], saturated loops cannot be observed even at the maximal electric field that can be offered by the apparatus. As shown in the inset of Fig. 3b, the remanent polarization is enhanced in the BFON films compared with that of the BFOO films at the same measuring electric field.

In order to identify the origins of the different properties for the BFON and BFOO films, the contents of Fe²⁺ ions and oxygen vacancies are analyzed using the XPS technique. Fe 2p XPS spectra of the two films are shown in Fig. 4a. The binding energy of Fe 2p_{3/2} is expected to be 710.7 eV for Fe³⁺ and 709.3 eV for Fe²⁺. However, as shown in Fig. 4a, an asymmetric broad band at about 709.9 eV is identified for the two films annealed in different atmospheres, which indicates that the oxidation state of Fe in our films is the coexistence of both Fe³⁺ and Fe²⁺. In fact, the presence of Fe²⁺ is unavoidable during the high-temperature process [8]. For each of the spectra, the Fe 2p_{3/2} band is divided into two subbands centered at 709.3 eV and 710.7 eV, as shown by the solid lines in Fig. 4a. By calculating the relative integral intensity of the Fe²⁺ peak to the whole peak, the percentage of Fe²⁺ to the entire Fe component is calculated, which is about 29.8% for the BFON films, while it is 34.2% for the BFOO films.¹ This demonstrates that more Fe ions are maintained at +3 valence in the BFON films. In Fig. 4b, the O 1s peak can also be fitted into two peaks. The lower binding energy around 529.1 eV, denoted by O_[1], represents the oxygen in the lattice, while the

¹Although the exact fraction of Fe²⁺ ions may fluctuate for the films fabricated at different times, the Fe²⁺ fraction is always smaller in the BFON films than that of the BFOO films.

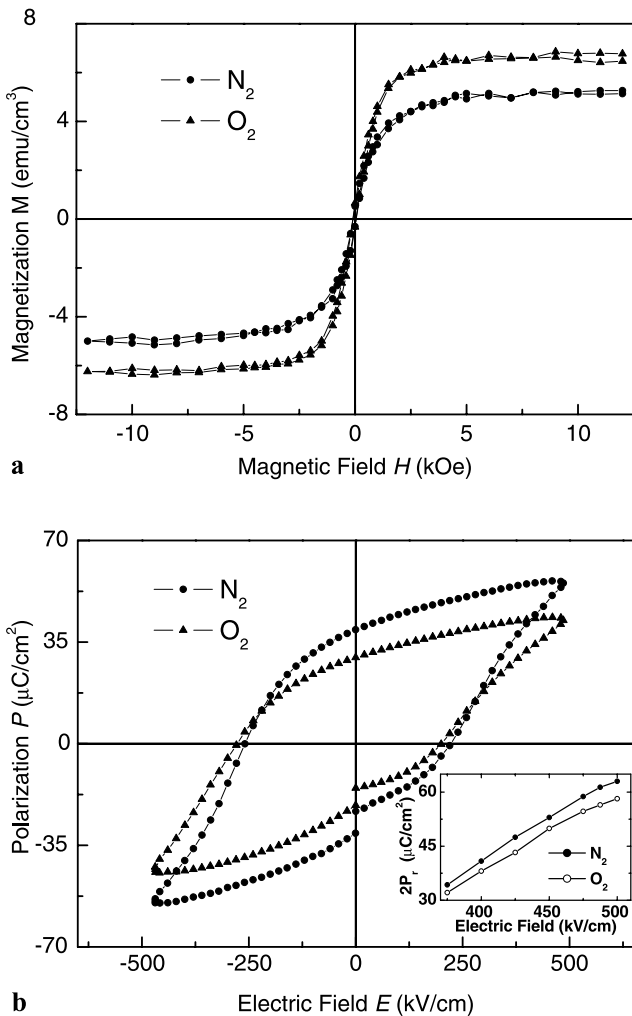


Fig. 3 Room-temperature **a** in-plane magnetization-field curves and **b** ferroelectric hysteresis loops of the two films annealed in different atmospheres. The *inset* in **b** shows the remanent polarization as a function of the maximum electric field. The measuring frequency of the ferroelectric hysteresis loops is 6 kHz

higher binding energy around 530.9 eV, denoted by O_[2], is assigned to absorbed oxygen species, which is related to the presence of oxygen vacancies [17, 18]. The relative amount of oxygen vacancies can be estimated by $I_{O[2]}/I_{O[1]}$ (I_O represents the integral intensity of the corresponding peak). When the annealing atmosphere changes from O₂ to N₂, $I_{O[2]}/I_{O[1]}$ increases from 0.48 to 0.62, which implies that more oxygen vacancies are involved in the BFON films.

For BFO, it was considered that the increased amount of Fe²⁺ ions should be accompanied with that of oxygen vacancies so as to reach charge balance. However, here a decreased Fe²⁺ fraction and an increased amount of oxygen vacancies are obtained simultaneously in our BFON films, which may be related with nitrogen incorporation. As pointed out for BaTiO₃, SrZrO₃ and HfO₂ [19–21], a small percentage of O²⁻ anions can be substituted by N³⁻ when

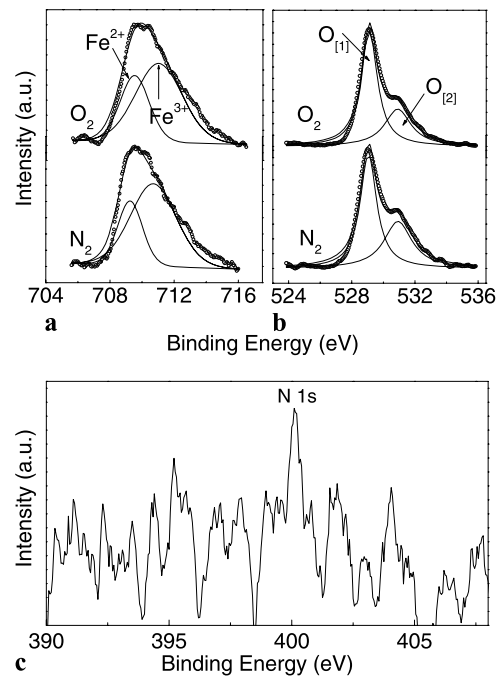
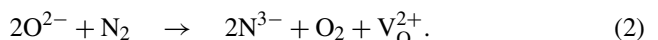


Fig. 4 XPS spectra of **a** Fe 2p_{3/2} and **b** O 1s for the BFOO and BFON films. The solid lines are the fitting curves. **c** XPS spectrum of N 1s electrons for the BFON films

annealing in N₂ or NH₃ atmosphere. In the BFON films, the incorporation of nitrogen into the O²⁻ sublattice is also possible, and a weak N 1s peak at about 400 eV is detected in the XPS spectrum (Fig. 4c). The related additional negative charges could be compensated according to the following reactions:



Here, V_O^{2+} represents the oxygen vacancies. For formula (1), it is clear that nitrogen incorporation would result in a decreased Fe²⁺ fraction, which is consistent with the result obtained from Fig. 4a. In formula (2), Fe ions do not directly participate in the reaction; when two N³⁻ anions build into the sublattice, site balance requires the removal of two oxygen anions, and charge balance demands an additional oxygen vacancy [20]. Either of the above processes possibly happens. As a result, a smaller Fe²⁺ fraction while more oxygen vacancies are involved in the BFON films.

The different macroscopic ferroelectric and magnetic properties in the two kinds of films (Fig. 3) can thus be explained as follows: first, the reduced magnetization of BFON. Since the magnetism of BFO is related to the amount of Fe²⁺ ions [22, 23], the decreased macroscopic magnetization in the BFON films may result from the decreased Fe²⁺ fraction. Second, the enhanced remanent polarization (P_r) of BFON. It is known that both the oxygen vacancies and

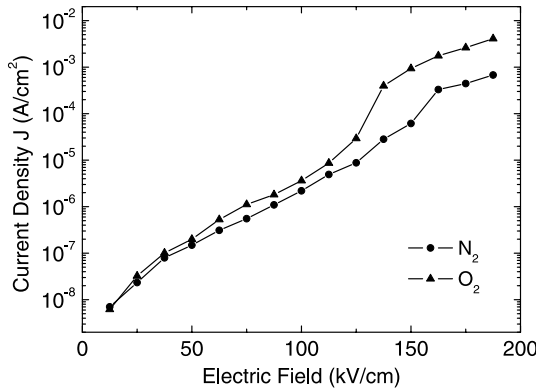


Fig. 5 Leakage current density of the BFON and BFOO films

the valence fluctuation of Fe ions could affect P_r . Oxygen vacancies with sufficient hopping mobility could assemble into an extended structure in the vicinity of domain walls, so as to impede the nucleation of new domains and cause strong domain pinning; thus, this would lead to a decrease of P_r [24]. The incorporation of Fe^{2+} ions (with radius larger than that of Fe^{3+} ions) would introduce a local structural distortion of the oxygen octahedron [25], which possibly results in a deterioration of the polarization since the ferroelectric properties of BFO are closely related to the stability of the FeO_6 cages. Therefore, the enhanced remanent polarization in the BFON films is probably also dominated by the reduced Fe^{2+} fraction and in turn the enhanced stability of the oxygen octahedron, although the increased amount of oxygen vacancies would tend to decrease the polarization of the films. To sum up, at room temperature, the reduced magnetism and improved ferroelectricity of the BFON films compared with that of the BFOO films are predominated by the reduced Fe^{2+} fraction.

Figure 5 shows the dc leakage properties of BFON and BFOO films. As for the BFO-based thin films, the causes of a rather high leakage current have been attributed to the presence of Fe^{2+} ions and the oxygen nonstoichiometry [7, 8]. For the BFON films, more oxygen vacancies should lead to an increased leakage current. However, as shown in Fig. 5, the leakage current density (J) for the BFON films is actually smaller than that of the BFOO films, thus, we consider that oxygen vacancies are not the main contributor to the room-temperature leakage current. Since the electron hopping between Fe^{2+} and Fe^{3+} ions will increase the leakage current, the smaller J in the BFON films can also be attributed to the decreased Fe^{2+} fraction.

The role of Fe^{2+} ions can be further confirmed by the room-temperature dielectric measurements. Figure 6 shows the frequency-dependent dielectric constant ϵ_r and the loss factor $\tan \delta$ of the two kinds of films. The two films present a similarly weak frequency dependence of dielectric characters; besides, both ϵ_r and $\tan \delta$ of the BFOO films are larger

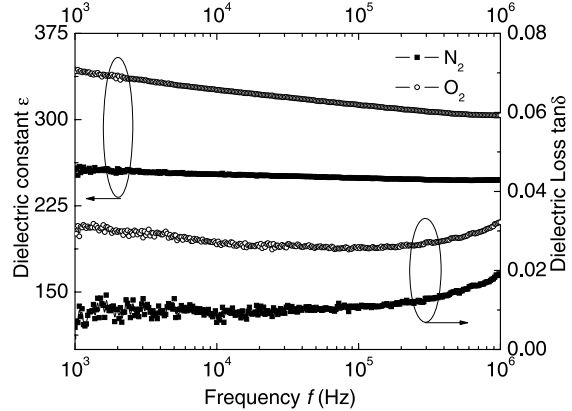


Fig. 6 Frequency dependence of dielectric constant and loss measured at room temperature for the BFON and BFOO films

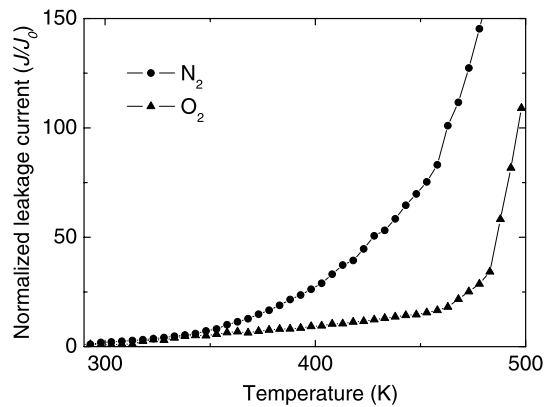


Fig. 7 Temperature dependence of normalized leakage current (J/J_0) for the BFON and BFOO films, measured at an electric field of 100 kV/cm. J_0 is the corresponding leakage current measured at room temperature

than those of the BFON films in the whole measuring frequency range. It is known that the contribution of electrons to the dielectric properties is independent of the measuring frequency, while other contributions, such as those from oxygen vacancies and interfacial polarization, are generally strongly dependent on the frequency. It is thus reasonable to believe that the increased ϵ_r and $\tan \delta$ of the BFOO films in the whole measuring frequency range probably come from the enhanced contribution of hopping electrons induced by the increased Fe^{2+} fraction.

Though all the above results suggest the predominant effect of the Fe^{2+} fraction variation related with nitrogen incorporation on the properties of the films, the influence of oxygen vacancies arises at elevated temperatures. As shown in Fig. 7, unlike the response of J to an electric field (Fig. 5), the leakage current of the BFON films increases more quickly with increasing temperature at a fixed electric field, which may be related to the activation of the conduction mechanism related with oxygen vacancies at high temperature. The activation energy is about 0.1 eV for the

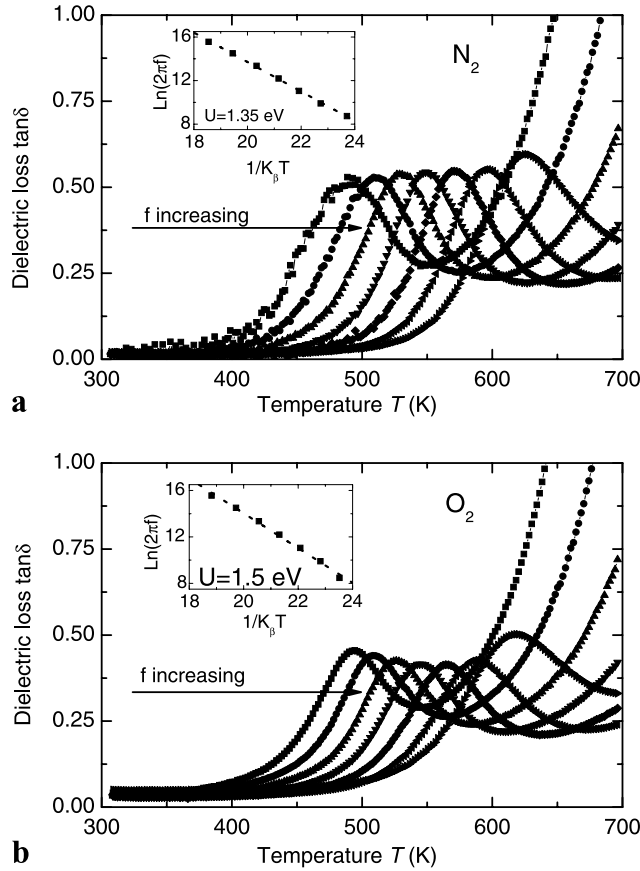


Fig. 8 Temperature-dependent dielectric loss $\tan \delta$ for **a** the BFON and **b** the BFOO films measured at various frequencies 10^3 , $10^{3.5}$, 10^4 , $10^{4.5}$, 10^5 , $10^{5.5}$ and 10^6 Hz. The insets in **a** and **b** show linear fit results by the Arrhenius law for the BFON and BFOO films, respectively

electrons [26] and about 1 eV for oxygen vacancies [27]. At room temperature, the electron hopping between Fe^{2+} and Fe^{3+} ions dominates the leakage current as aforementioned, while, as the temperature increases, the oxygen vacancies might be thermally activated, and so contribute more to the leakage current. Compared with the BFOO films, more oxygen vacancies are involved in the BFON films; therefore, a more strongly temperature-dependent leakage current is observed.

The perspective that oxygen vacancies can be activated at elevated temperature might be further confirmed by the temperature-dependent dielectric loss measurement. As shown in Fig. 8, wide and prominent relaxation peaks appear in the temperature range 450–650 K for the films annealed in different atmospheres. Though the loss factor $\tan \delta$ of the BFON films is smaller at room temperature, its relaxation peak is higher compared with that of the BFOO films. We have pointed out in our previous work [15] that the possible causes for the dielectric anomaly of BFO/BLT films are the formation of polar nanoregions due to the presence of Fe^{2+} , the coupling of electric and magnetic order parameters, and the oxygen vacancies. Here, the magnetoelectricity coupling

can probably be excluded since it is related to phase transition but not relaxation [28]. As for the oxygen vacancies and Fe^{2+} ions, a detailed analysis is given below to see which is the main contributor to the dielectric loss relaxation process. First, according to the point defect relaxation theory [29], the higher dielectric loss peak in the BFON films suggests that the concentration of relaxation units is larger. Since more oxygen vacancies are involved in the BFON films, the main relaxation units might be related to oxygen vacancies. Second, as shown in the insets of Fig. 8, the activation energy of the relaxation units, fitted by the Arrhenius law, is comparable with that reported for oxygen vacancies [27]. Third, the activation energy increases from 1.35 eV to 1.5 eV when the annealing atmosphere changes from N₂ to O₂, which is consistent with what is indicated by Li et al. [29] that the activation energy would increase with the decreasing concentration of the relaxation units (here fewer oxygen vacancies in the BFOO films) due to the collective effect. Therefore, the oxygen vacancy is most probably the main contributor to the relaxation process.

4 Conclusions

Two kinds of BFO/BLT films were prepared with the BFO layer being annealed in different atmospheres (N₂ or O₂). Based on XPS analysis, it was found that the nitrogen incorporation induced a decreased Fe^{2+} fraction and an increased content of oxygen vacancies in the films. Thus, in the BFON films at room temperature, predominated by the reduced Fe^{2+} fraction, lower leakage current and dielectric loss, better ferroelectric property while a reduced magnetization were observed. However, the oxygen vacancies could be thermally activated at elevated temperature. As a result, more strongly temperature-dependent leakage current and a higher dielectric relaxation peak were observed for the BFON films with more oxygen vacancies.

In another words, compared with O₂ annealing atmosphere, N₂ is good for the room-temperature electric properties, but not for the temperature stability of the BFO films. So, N₂ annealing atmosphere may not be the best choice. Moreover, Yun et al. [12] and Iakovlev et al. [14] reported that the BFO films annealed in air show the formation of secondary phases and poor electric properties. It seems that some other types of annealing atmosphere, such as N₂O, etc., may be better alternatives.

Acknowledgements This work was supported by the National Science Foundation (No. 50672034), the 973 Project of MOST (Nos. 2006CB921804 and 2009CB929501), NCET-06-0443, NFFTBS (No. J0630316) and the Jiangsu Natural Science Foundation (No. BK2007128).

References

1. H. Schmid, *Ferroelectrics* **162**, 317 (1994)
2. W. Eerenstein, N.D. Mathur, J.F. Scott, *Nature (London)* **442**, 759 (2006)
3. T.J. Park, G.C. Papaefthymiou, A.J. Viescas, A.R. Moodenbaugh, S.S. Wong, *Nano Lett.* **7**, 766 (2007)
4. N.A. Spaldin, M. Fiebig, *Science* **309**, 391 (2005)
5. T. Lottermoser, T. Lonkai, U. Amann, D. Hohlwein, J. Ihringer, M. Fiebig, *Nature (London)* **430**, 541 (2004)
6. C. Ederer, N.A. Spaldin, *Phys. Rev. B* **71**, 224103 (2005)
7. M.M. Kumar, V.R. Palkar, K. Srinivas, S.V. Suryanarayana, *Appl. Phys. Lett.* **76**, 2764 (2000)
8. F.Z. Huang, X.M. Lu, W.W. Lin, X.M. Wu, Y. Kai, J.S. Zhu, *Appl. Phys. Lett.* **89**, 242914 (2006)
9. V.R. Palkar, J. John, R. Pinto, *Appl. Phys. Lett.* **80**, 1628 (2002)
10. S. Nomura, K. Doi, *Jpn. J. Appl. Phys.* **9**, 716 (1970)
11. K.Y. Yun, M. Noda, M. Okuyama, *Appl. Phys. Lett.* **83**, 3981 (2003)
12. K.Y. Yun, M. Noda, M. Okuyama, *J. Korean Phys. Soc.* **42**, S1153 (2003)
13. V.R. Singh, A. Dixit, A. Garg, D.C. Agrawal, *Appl. Phys. A* **90**, 197 (2008)
14. S. Iakovlev, C.H. Solterbeck, M. Kuhnke, M. Es-Souni, *J. Appl. Phys.* **97**, 094901 (2005)
15. F.Z. Huang, X.M. Lu, W.W. Lin, W. Cai, X.M. Wu, Y. Kan, H. Sang, J.S. Zhu, *Appl. Phys. Lett.* **90**, 252903 (2007)
16. W. Tian, V. Vaithyanathan, D.G. Schlom, Q. Zhan, S.Y. Yang, Y.H. Chu, R. Ramesh, *Appl. Phys. Lett.* **90**, 172908 (2007)
17. C.M. Pradier, C. Hinnen, *J. Mater. Sci.* **33**, 3187 (1998)
18. A.B. Hungrfa, A. Martinez-Arias, M. Fernandez-Garcia, A. Iglesias-Juez, A. Guerrero-Ruiz, J.J. Calvino, J.C. Conesa, J. Sorria, *Chem. Mater.* **15**, 4309 (2003)
19. X.B. Lu, G.H. Shi, J.F. Webb, Z.G. Liu, *Appl. Phys. A* **77**, 481 (2003)
20. T. Brauniger, T. Muller, A. Pampel, H.P. Abicht, *Chem. Mater.* **17**, 4114 (2005)
21. B. Sen, H. Wong, B.L. Yang, A.P. Huang, P.K. Chu, V. Filip, C.K. Sarkar, *Jpn. J. Appl. Phys.* **46**, 3234 (2007)
22. W. Eerenstein, F.D. Morrison, J. Dho, M.G. Blamire, J.F. Scott, N.D. Mathur, *Science* **307**, 1203a (2005)
23. J. Wang, A. Scholl, H. Zheng, S.B. Ogale, D. Viehland, D.G. Schlom, N.A. Spaldin, K.M. Rabe, M. Wuttig, L. Mohaddes, J. Neaton, U. Waghmare, T. Zhao, R. Ramesh, *Science* **307**, 1203b (2005)
24. W. Wang, S.P. Gu, X.Y. Mao, X.B. Chen, *J. Appl. Phys.* **102**, 024102 (2007)
25. X.D. Qi, J.H. Dho, M. Blamire, Q.X. Jia, J.S. Lee, S. Foltyn, J.L. MacManus-Driscoll, *J. Magn. Magn. Mater.* **283**, 415 (2004)
26. R. Manjula, V.R.K. Murthy, J. Sobhanadri, *J. Appl. Phys.* **59**, 2929 (1986)
27. J.F. Scott, *Ferroelectric Memories* (Springer, Berlin, 2000)
28. L. Benguigui, *Solid State Commun.* **11**, 825 (1972)
29. W. Li, K. Chen, Y.Y. Yao, J.S. Zhu, Y.N. Wang, *Appl. Phys. Lett.* **85**, 4717 (2004)